

1 **Investigating Recent Changes in MJO Precipitation**
2 **and Circulation in Two Reanalyses**

3 **Wei-Ting Hsiao¹, Eric D. Maloney¹, and Elizabeth A. Barnes¹**

4 ¹Department of Atmospheric Science, Colorado State University, Fort Collins, Colorado, USA

5 **Key Points:**

- 6 • Non-monotonic increases in MJO circulation and precipitation amplitude over the
7 period of 1981-2018 are found in ERA5 and MERRA-2.
8 • Decrease in the ratio of MJO circulation to precipitation amplitudes is detected
9 and is explained by the weak-temperature-gradient theory.

Corresponding author: Wei-Ting Hsiao, WeiTing.Hsiao@colostate.edu

Abstract

Recent work using CMIP5 models under RCP8.5 suggests that individual multimodel-mean changes in precipitation and wind variability associated with the Madden-Julian oscillation (MJO) are not detectable until the end of the 21st century. However, a decrease in the ratio of MJO circulation to precipitation anomaly amplitude is detectable as early as 2021-2040, consistent with an increase in dry static stability as predicted by weak-temperature-gradient balance. Here, we examine MJO activity in two reanalyses (ERA5 and MERRA-2) and find a detectable decrease in the ratio of MJO circulation to precipitation anomaly amplitude over the observational period, consistent with the change in dry static stability. MJO wind and precipitation anomalies individually increase in strength relative to the start of the record, but these changes are non-monotonic. These results suggest that weak-temperature-gradient theory may be able to help explain changes in MJO activity in recent decades.

Plain Language Summary

A recent study examined future projected changes in precipitation and wind strength associated with the Madden-Julian oscillation (MJO) in a set of anthropogenically-forced warming simulations. While they showed that changes in the amplitude of individual MJO-related variables are not detectable until the end of the 21st century, they also demonstrated that a decrease in the ratio of MJO wind to precipitation anomaly amplitude is detectable as early as 2021-2040. To examine whether these MJO changes found in climate models are realistic, changes to MJO variability are assessed in two observational products, and we find that a similar decrease in the ratio of MJO wind to precipitation strength is detectable over 1981-2018. In addition, the strength of MJO circulations and precipitation both increase relative to the start of the record, although these changes do not increase consistently from year to year. Our results suggest that the change in MJO activity in recent decades may be a detectable climate warming signal.

1 Introduction

The Madden-Julian oscillation (MJO; Madden & Julian, 1971, 1972) is the dominant mode of large-scale tropical precipitation variability on intraseasonal timescales. MJO activity impacts the occurrence of extreme weather events not only in tropics, but also at higher latitudes due to its remote teleconnections (Zhang, 2013). Because of its ability to modulate weather across the globe, with clear implications for lives and property, extensive research is being conducted about the MJO, with increasing attention given to the evolution of the MJO under anthropogenic warming (Maloney et al., 2019). As global temperatures rise, MJO activity is expected to be impacted by competing effects, making the projections of the MJO difficult. For example, an increased basic state vertical moisture gradient in the lower troposphere increases the efficiency with which vertical motion moistens the atmosphere, leading to a strengthening of MJO-associated convection (Arnold et al., 2013; Holloway & Neelin, 2009). In contrast, an increased dry static stability decreases the efficiency by which diabatic heating induces vertical motion (Knutson & Manabe, 1995; Sherwood & Nishant, 2015; Sobel & Bretherton, 2000), which would tend to weaken MJO-associated convection (e.g. Chikira, 2014). Future projections from most global climate models (GCMs) suggest an increase in the amplitude of MJO precipitation under anthropogenic warming, although MJO circulation anomalies weaken, or at least increase less than precipitation (Maloney et al., 2019). Analysis of the reconstructed historical record from instrumental observations and reanalysis shows positive trends of MJO amplitude over the 20th century in surface pressure and precipitation (Oliver & Thompson, 2012) and in the late 20th century in zonal winds (Jones & Carvalho, 2006; Slingo et al., 1999). However, other studies have found no trend in boreal-wintertime MJO

59 amplitude from the 1980s to the 2000s when using an outgoing longwave radiation-related
60 metric (Tao et al., 2015).

61 Recent evidence suggests that the MJO may undergo structural changes with warm-
62 ing and differences in intensification rate in its associated precipitation and circulation
63 components. Such changes would be important because teleconnections generated by upper-
64 level divergence associated with MJO convection have a large impact on extratropical
65 weather and its predictability (Ferranti et al., 1990; Zhang, 2013). Instead of examin-
66 ing the amplitude of the MJO with a single variable, Maloney and Xie (2013) and Wolding
67 and Maloney (2015) suggest that in the deep tropics where the weak-temperature-gradient
68 (WTG) approximation holds (Sobel & Bretherton, 2000), the amplitude ratio of verti-
69 cal velocity to precipitation associated with the MJO is constrained by dry static sta-
70 bility. Since the temperature profile in the free tropical troposphere roughly follows a
71 moist adiabat determined by convective adjustment in tropical convecting regions (Knutson
72 & Manabe, 1995), the dry static stability profile may be constrained by future SST warm-
73 ing, thus providing a constraint on future MJO behavior.

74 A recent study found that the ratio of MJO-associated circulation to precipitation
75 amplitude follows WTG balance in anthropogenic warming simulations (Bui & Maloney,
76 2019). The WTG approximation can be applied to the thermodynamic equation to pro-
77 duce the following approximate balance in the tropical free troposphere, where horizon-
78 tal temperature gradients are small (Sobel & Bretherton, 2000),

$$79 \quad \omega \frac{\partial s}{\partial p} \approx Q_1 \quad (1)$$

80 where ω is the vertical pressure velocity, s the dry static energy (DSE), and Q_1 the ap-
81 parent heat source (Yanai et al., 1973). Note that all variables represent the large-scale
82 area average. If it is further assumed that precipitation is proportional to Q_1 in MJO
83 convective regions, and that the vertical structure of Q_1 is not changed (Maloney & Xie,
84 2013), it follows that at a given level:

$$85 \quad \Delta \left(\frac{\omega}{P} \right) \propto \Delta \left(\frac{\partial s}{\partial p}^{-1} \right) \quad (2)$$

86 where P is the surface precipitation rate, and Δ denotes the relative change from a refer-
87 ence state to a new state. Bui and Maloney (2019) examined GCM simulations forced
88 by Representative Concentration Pathway 8.5 (RCP8.5) in a subset of models partic-
89 ipating in the Coupled Model Intercomparison Project 5 (CMIP5) that simulated real-
90 istic MJOs. While the amplitude changes of MJO precipitation and vertical velocity were
91 individually not detectable until 2080, the *ratio* of MJO vertical velocity to precipita-
92 tion amplitude showed detectable decreases as early as 2021-2040. Consistent with WTG
93 balance and the proportionality of precipitation to Q_1 , the ratio of MJO vertical veloc-
94 ity to precipitation amplitude matches the change in dry static stability in the simula-
95 tions, implying that this theory could explain and predict the evolution of the MJO, even
96 in the observational record that has exhibited warming.

97 Following this work, we investigate the temporal evolution of MJO-related precip-
98 itation and circulation amplitude and their ratio in two reanalyses (ERA5 and MERRA-
99 2) to assess whether changes to the MJO can be detected in recent decades. Our pur-
100 pose is to determine whether WTG balance can explain changes in MJO activity in the
101 real world, which could help support projections of MJO under continued anthropogenic
102 warming.

103 2 Data and Methodology

104 Two reanalysis datasets spanning 1981-2018 are employed to assess changes in MJO
105 amplitude and the background environment in recent decades: the Modern-Era Retro-
106 spective analysis for Research and Applications version 2 (MERRA-2; Gelaro et al., 2017)

107 and the European Centre for Medium-Range Weather Forecasts re-analysis (ERA5; Hers-
 108 bach et al., 2020). The MERRA-2 and ERA5 datasets have spatial (temporal) resolu-
 109 tions of $0.5^\circ \times 0.625^\circ$ (three hours) and $0.25^\circ \times 0.25^\circ$ (one hour), respectively. For the
 110 purpose of investigating large-scale dynamics, all variables are re-gridded to have a com-
 111 mon horizontal spatial resolution of $2.5^\circ \times 2.5^\circ$. Vertical pressure velocity and precip-
 112 itation are averaged into daily means, and temperature and DSE are originally obtained
 113 as monthly means. Wolding and Maloney (2015) imply that to good approximation the
 114 slowly varying background DSE gradient is appropriate to use in (1) for determining the
 115 dominant WTG MJO balance. While the precipitation data in both reanalyses is model-
 116 generated and comes with substantial caveats, inhomogeneities in satellite-observed pre-
 117 cipitation over the tropics make it difficult to use to detect climate trends (e.g. Yin et
 118 al., 2004). Furthermore, the moisture budget in the reanalyses products is more inter-
 119 nally consistent, and thus, we focus on reanalysis precipitation for this work.

120 MJO activity is assessed by its associated precipitation and vertical pressure ve-
 121 locity amplitudes, with vertical pressure velocity at 400 hPa (ω_{400}) used given the top-
 122 heavy nature of convection in the MJO (Kiladis et al., 2005). Specifically, the occurrence
 123 of an MJO event is defined as when the magnitude of the outgoing-longwave-radiation-
 124 based MJO index (OMI; downloaded from <https://www.psl.noaa.gov/mjo/mjoindex/omi.1x.txt>;
 125 see Kiladis et al., 2014, for definition) exceeds 1.0. Note that we split our analysis into
 126 19-year periods, and so OMI is normalized within each time period (as in Bui & Mal-
 127 oney, 2019) to reflect possible changes in variance of outgoing longwave radiation fields.
 128 Boreal winter (November to April) MJO composites for each of its eight phases are then
 129 generated for 30-90 day bandpass filtered variables as is commonly done in the MJO lit-
 130 erature (e.g. Kiladis et al., 2014). Amplitudes of MJO precipitation and ω_{400} for each
 131 location are calculated as the root-mean-square values across the composites of the eight
 132 MJO phases.

133 Boreal winter averages derived from monthly means of temperature and DSE are
 134 used to assess the background environment changes that could impact MJO activity. Dry
 135 static stability at 400 hPa is computed as the vertical gradient of DSE between 350 hPa
 136 and 450hPa.

137 Our focus is on the time evolution of the amplitudes of MJO precipitation and ω_{400}
 138 in the Indo-Pacific warm pool region (the IPWP region; 15°S - 15°N , 60°E - 180°) where
 139 the MJO is most active, as shown in the boxed region in Figure 1. Area-averaged MJO
 140 precipitation and ω_{400} amplitudes over the IPWP region are used as metrics to quan-
 141 tify overall MJO activity.

142 Composites obtained from 19-year running windows are extensively used in this
 143 study, similar to the averaging window length of 20 years used in Bui and Maloney (2019).
 144 This window length is chosen to reduce noise from decadal variations, but also to retain
 145 enough data points to show the time evolution of MJO activity. Since the entire time
 146 period analyzed is 38 years, the first and the last 19 years of the record are the only two
 147 periods that are truly independent, and we refer to these as the *early period* (1981-1999)
 148 and the *late period* (2000-2018). The conclusions in this study are not sensitive to the
 149 choice of window length used between 15 years and 25 years (Figure S1).

150 3 Results

151 First, we explore the spatial structure of MJO activity in the two reanalyses. The
 152 amplitude of MJO precipitation and ω_{400} maximize in the IPWP region (Figures 1a-d)
 153 in both reanalyses during the early period. The changes in MJO precipitation and ω_{400}
 154 amplitude between the late period and the early period have rich spatial structures, which
 155 are similar between the reanalyses (Figures 1e-h). Increases in both amplitudes occur
 156 to the south of India, at the southern edge of the Pacific warm pool, and near the Philip-

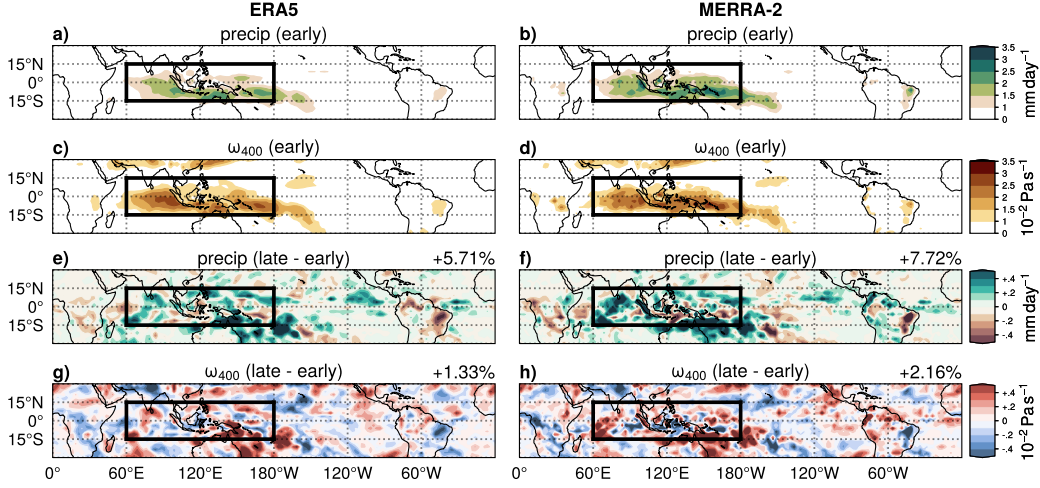


Figure 1. The boreal winter composite amplitudes of (a, b) MJO precipitation and (c, d) MJO ω_{400} during the early period (1981-1999), and (e-h) their difference from the late period (2000-2018), from (left column) ERA5 and (right column) MERRA-2. The black rectangle encloses the Indo-Pacific warm pool region, and the percentage values shown in the upper right corners of (e-h) are the area-averaged relative changes over the region.

157 pines. Decreases in both amplitudes occur near 5°S over the Maritime Continent. The
 158 regions of large amplitude of the MJO do not change substantially between the early and
 159 late period, allowing us to assess the temporal change in MJO activity within the IPWP
 160 region. The area-averaged amplitude of MJO precipitation and ω_{400} in the IPWP region
 161 both show increases in the late period relative to the early period with precipitation in-
 162 tensifying by 5.6% in ERA5 and 7.6% in MERRA-2, and ω_{400} intensifying by 1.2% in
 163 ERA5 and 2.1% in MERRA-2. Most important for this study, MJO precipitation ampli-
 164 tude intensifies more than MJO ω_{400} amplitude in both reanalyses, although MJO ac-
 165 tivity in MERRA-2 is strengthened slightly more than in ERA5.

166 The 19-year running area-averaged MJO precipitation and ω_{400} amplitude in the
 167 IPWP region increase between the early and the late periods of the record, while the am-
 168 plitude in MERRA-2 exhibit larger changes than those in ERA5. However, both reanal-
 169 yses demonstrate qualitatively similar fluctuations in between: in the early 90s, both of
 170 the amplitudes rise quickly, followed by a plateau and then a slight decrease afterward
 171 (Figures 2a-b). The strengthening of the boreal-wintertime MJO activity during the late
 172 20th century is consistent with previous studies examining observed zonal wind changes
 173 at 200 hPa and 850 hPa (Jones & Carvalho, 2006)). Moreover, both reanalyses agree that
 174 throughout the record, MJO precipitation amplitude shows larger positive changes than
 175 MJO ω_{400} amplitude.

176 While we attempted to explain the fluctuating pattern in MJO precipitation and
 177 ω_{400} amplitude, we could find no obvious connections between them and interannual to
 178 decadal variability in surface air temperature. The evolution of surface air temperature
 179 in the IPWP region (Figure S2b) and its evolution relative to the whole tropics (Figure
 180 S2c) do not resemble the variability in the MJO amplitude time series, which have dif-
 181 ferent trends from the early 90s onward (Figures 2a-b). Commonly used Pacific SST in-
 182 dices that capture interannual to decadal variability also do not show similar variabil-
 183 ity to the MJO amplitude time series (compare Figures 2a-b with Figure S3 SST-indices).

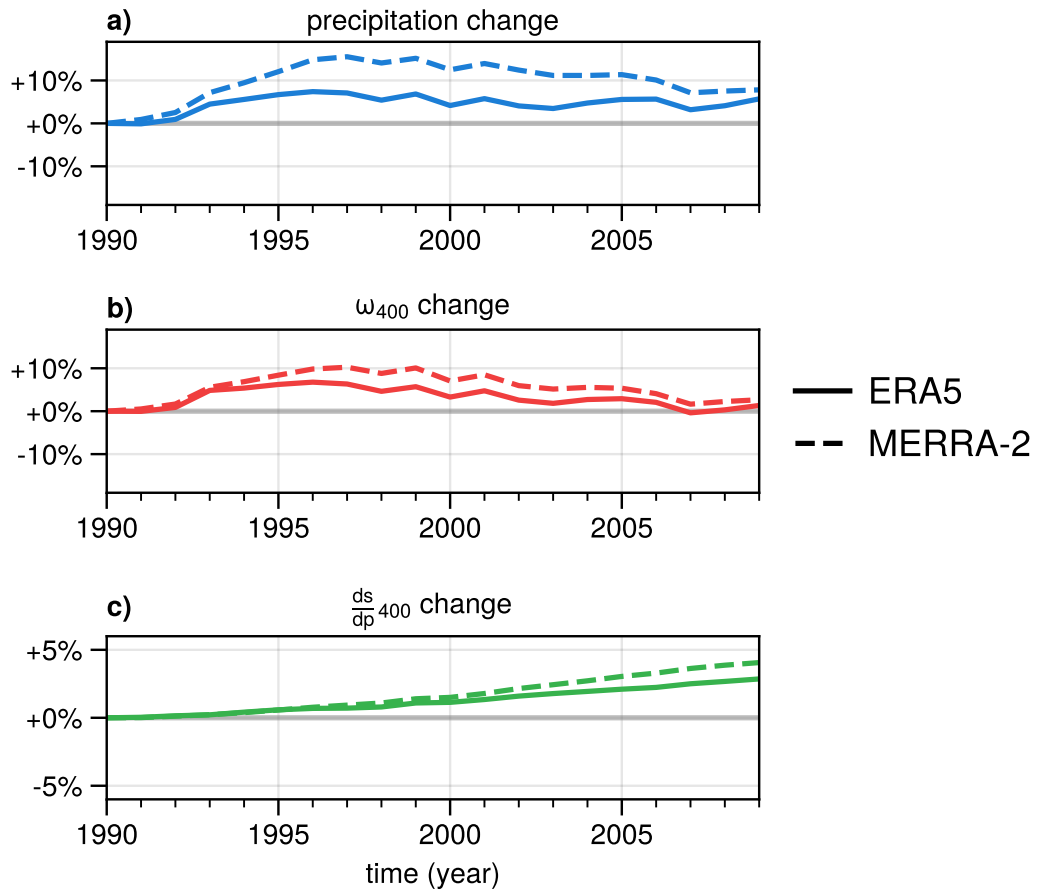


Figure 2. Relative change in 19-year wintertime running composites of (a) MJO precipitation amplitude, (b) MJO ω_{400} amplitude, and (c) dry static stability at 400 hPa with respect to the early period. The x-axis denotes the central years of the associated time window, for example, 2000 denotes the period of 1991-2009. The y-axis denotes the relative change to the early period.

184 To sum up, both MJO precipitation and ω_{400} amplitude increase from the early
 185 period to the late period in the IPWP region in both reanalyses, although the time evo-
 186 lution is non-monotonic and the amplitude of the change varies between the reanalyses.
 187 The timeseries of the amplitudes are not easily explained by tropical SST variability. How-
 188 ever, a robust result common among different time periods and reanalyses is that the
 189 increase in MJO precipitation amplitude is always stronger than in MJO ω_{400} amplitude,
 190 consistent with what WTG balance would predict based on the increasing tropical static
 191 stability with SST warming observed in recent decades (Figure 2c; see also e.g. Sherwood
 192 & Nishant, 2015). We explore this contention more below.

193 Given a change in dry static stability, the theoretical change in the ratio of MJO
 194 ω_{400} to precipitation amplitude can be computed if one assumes that WTG balance holds
 195 (equation 1, 2). Previous modeling studies have shown good agreement between static
 196 stability changes and this ratio when applied to MJO-associated wind and precipitation
 197 variance (Maloney & Xie, 2013; Wolding & Maloney, 2015; Wolding et al., 2016; Bui &
 198 Maloney, 2018). As the climate system warms, tropical dry static stability increases in
 199 the troposphere because the atmospheric profile in the deep tropics roughly follows a moist
 200 adiabat set by the surface temperature in convecting regions (Knutson & Manabe, 1995).
 201 Because surface temperature has increased since 1981 (Figure S2a), equation (2) would
 202 argue for a greater change in MJO precipitation amplitude compared to MJO ω_{400} am-
 203 plitude.

204 Figure 3 displays the temporal evolution of the inverse of dry static stability and
 205 the ratio of MJO ω_{400} to precipitation amplitude (MJO ω_{400}/P ; see equation 2) in the
 206 two reanalyses. The grey diagonal line denotes the predicted theoretical relationship be-
 207 tween MJO ω_{400}/P and inverse static stability assuming WTG theory holds and the ver-
 208 tical structure of the MJO remains unchanged. Between the late period and the early
 209 period (the two outlined endpoints), the decrease of the inverse of dry static stability is
 210 2.8% in ERA5 and 4.0% in MERRA-2, and the decrease of MJO ω_{400}/P is 4.2% in ERA5
 211 and 4.9% in MERRA-2. Consistent with WTG theory, MJO ω_{400}/P and the inverse of
 212 dry static stability show comparable decreases between the early period (1981-1999) and
 213 the late period (2000-2018). Agreement is also good in ERA5 for interim periods, espe-
 214 cially until about 2000 (Figure 3a). Considering the complicated temporal evolution of
 215 MJO precipitation and ω_{400} amplitude (Figure 2), WTG balance provides a reasonable
 216 explanation for the evolution of MJO ω_{400}/P over the past 38 years, especially when con-
 217 sidering the start and end of the record (Figure 3).

218 As many MJO studies use zonal wind amplitude as a metric of MJO activity (e.g.
 219 Slingo et al., 1999; Jones & Carvalho, 2006), we also examine the amplitude of MJO 850
 220 hPa zonal wind (u_{850}) for reference. The evolution of the ratio of MJO circulation to pre-
 221 cipitation amplitude is defined here using u_{850} (MJO u_{850}/P). Although using u_{850} is
 222 not a direct application of WTG balance in equation (2), the amplitude of horizontal ve-
 223 locity should scale with vertical velocity through divergence if the vertical structure doesn't
 224 change (Maloney & Xie, 2013). Under such conditions, we would expect a qualitatively
 225 similar decrease in the ratio of MJO u_{850} to precipitation amplitude. Figure S4 shows
 226 that u_{850} amplitude relative to precipitation does decrease in a qualitatively similar way,
 227 although with stronger decreases relative to P than for ω_{400} .

228 Differences between the two reanalyses are notable in Figure 3. In ERA5, equa-
 229 tion (2) explains the change in MJO ω_{400}/P very well until 2000 and then starts to mod-
 230 estly underestimate the change after 2000; in MERRA-2, equation (2) overestimates the
 231 decrease in MJO ω_{400}/P in the intervening periods but works well for the two endpoints.
 232 MJO ω_{400}/P in MERRA2 shows stronger decreases than ERA5 during the interim pe-
 233 riod largely because it has a larger P amplitude change than ERA5. The exact reasons
 234 for differences between the two analyses are unclear, although they may depend on the
 235 different behavior of tropical convection simulated by the two reanalysis models. The
 236 differing dry static energy profiles changes between ERA5 and MERRA-2 for the IPWP

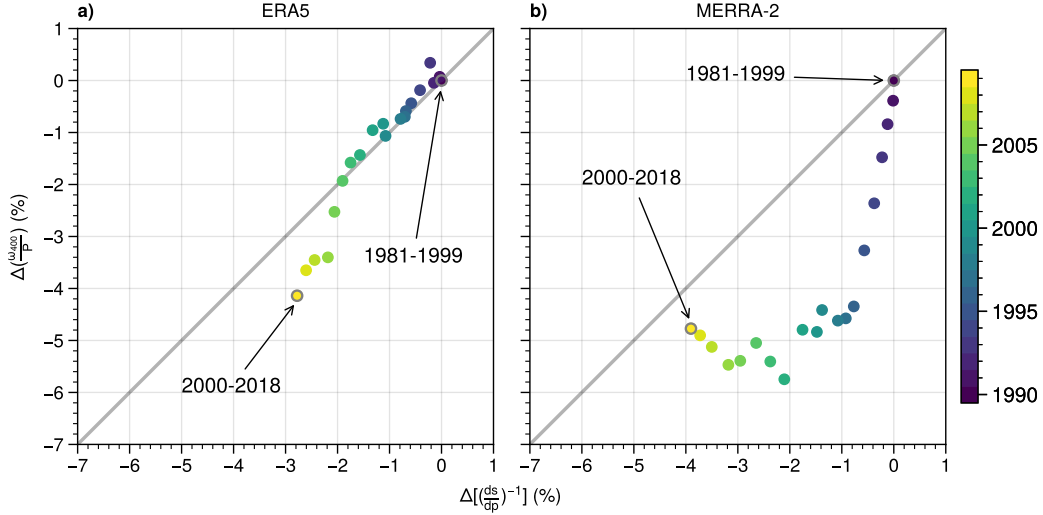


Figure 3. Relative change in (x-axis) the reciprocal of dry static stability at 400 hPa and (y-axis) the ratio of MJO ω_{400} to precipitation amplitude over the IPWP region between 19-year running windows and the early period. Colors indicate the central year of the running window. The grey diagonal line denotes the change in the ratio predicted by WTG balance assuming vertical heating structure is unchanged (equation 2). The first and the last points, which are independent, are emphasized by grey outlines.

237 region (Figures S5a-b) not only indicate differing static stability changes, but also cir-
 238 cumstantially suggest different changes to the convective heating structure between datasets
 239 given the regulation of tropical tropospheric temperature by convective heating. Such
 240 structure changes would affect how well the balance in equation (2) reflects equation (1),
 241 considering the assumption about the proportionality of P to Q_1 at 400 hPa. MERRA-
 242 2 exhibits more warming in the lower troposphere than ERA5, presumably associated
 243 with increased condensational heating and precipitation generation there, which would
 244 produce greater decreases in MJO ω_{400}/P than that expected by looking at the 400 hPa
 245 level in isolation. The rate of increase in low-level warming in MERRA-2 is particularly
 246 strong until the 19-year period centered on 1997, possibly consistent with the greater MJO
 247 precipitation amplitude increase in MERRA during that time than ERA5 (Figure 2),
 248 although translating mean state convective structure changes to those on subseasonal
 249 timescales should be done with care. While these arguments are suggestive, we leave a
 250 detailed investigation into the evolution of tropical convective structure through exam-
 251 ination of Q_1 to a future study.

252 4 Summary

253 The changes to MJO precipitation and ω_{400} amplitude from 1981 to 2018 are ex-
 254 amined in two reanalysis datasets, ERA5 and MERRA-2. Both amplitudes individually
 255 increase from the early period (1981-1999) to the late period (2000-2018) (Figure 1). How-
 256 ever, their temporal behavior is non-monotonic in that both amplitudes intensify from
 257 1981 to 1997 and slowly weaken or remain constant thereafter (Figure 2). Interannual-
 258 to-decadal surface temperature variability (Figure S2; Figure S3) shows no simple rela-
 259 tionship with this non-monotonic behavior in MJO activity changes.

260 When viewed together, amplitude changes of MJO precipitation are larger than MJO
 261 ω_{400} throughout the past four decades relative to the early period (1981-1999). A pref-

262 erential strengthening of MJO precipitation amplitude relative to MJO ω_{400} amplitude
 263 is predicted by WTG balance with a warming climate, in that increasing dry static stability
 264 in response to SST warming in recent decades makes vertical motion more efficient
 265 at compensating latent heat release in deep convective regions. The fractional amplitude
 266 changes in the ratio of MJO ω_{400} to precipitation between 1981-1999 and 2000-2018 ap-
 267 proximately match inverse dry static stability changes with climate warming, consistent
 268 with WTG balance (Figure 3).

269 While trends in both reanalyses appear to generally follow WTG balance, differ-
 270 ences exist in the behaviour of the two reanalyses. MJO precipitation and ω_{400} ampli-
 271 tude increases are larger in MERRA-2 than in ERA5, especially in intermediate peri-
 272 ods between the beginning and end of the record, although they show qualitatively sim-
 273 ilar time series variability. Decreases in MJO ω_{400}/P also fit the theoretical prediction
 274 based on the inverse of dry static stability better in ERA5 than in MERRA-2 across all
 275 19-year periods examined, and these differences may be associated with differences in
 276 the simulated structure of tropical deep convection, which remains a topic for further
 277 investigation.

278 The present paper provides a preliminary assessment of MJO activity changes over
 279 the past four decades that include both anthropogenic forcing and natural variability.
 280 Our results based on observations support those previously derived from climate mod-
 281 els (e.g. Bui & Maloney, 2019) suggesting that decreases in MJO ω_{400}/P occur as sur-
 282 face temperatures warm due to anthropogenic forcing. Nevertheless, discrepancies be-
 283 tween results from ERA5 and MERRA-2 leave lingering questions about the degree to
 284 which changes to the MJO can be explained by WTG theory alone in response to cli-
 285 mate warming. Further work using a broader set of observational data including trop-
 286 ical sounding and other in situ records are needed to affirm the validity of WTG theory
 287 for explaining MJO behavior.

288 Acknowledgments

289 The ERA5 reanalysis was generated using Copernicus Climate Change Service Informa-
 290 tion and the MERRA-2 reanalysis was generated using NASA GES DISC during 2019-
 291 2020. This research has been conducted as part of the NOAA MAPP S2S Prediction Task
 292 Force and supported by NOAA grant NA16OAR4310064. Work was also supported by
 293 NSF Grant AGS-1841754.

294 References

- 295 Arnold, N. P., Kuang, Z., & Tziperman, E. (2013, February). Enhanced MJO-like
 296 variability at high SST. *J. Clim.*, *26*(3), 988–1001.
- 297 Bui, H. X., & Maloney, E. D. (2018). Changes in Madden-Julian oscillation precip-
 298 itation and wind variance under global warming. *Geophys. Res. Lett.*, *45*(14),
 299 7148–7155.
- 300 Bui, H. X., & Maloney, E. D. (2019, November). Transient response of MJO precip-
 301 itation and circulation to greenhouse gas forcing. *Geophys. Res. Lett.*, *46*(22),
 302 13546–13555.
- 303 Chikira, M. (2014, February). Eastward-Propagating intraseasonal oscillation repre-
 304 sented by Chikira–Sugiyama cumulus parameterization. part II: Understanding
 305 moisture variation under weak temperature gradient balance. *J. Atmos. Sci.*,
 306 *71*(2), 615–639.
- 307 Ferranti, L., Palmer, T. N., Molteni, F., & Klinker, E. (1990, September). Tropical-
 308 Extratropical interaction associated with the 30–60 day oscillation and its
 309 impact on medium and extended range prediction. *J. Atmos. Sci.*, *47*(18),
 310 2177–2199.
- 311 Gelaro, R., McCarty, W., Suárez, M. J., Todling, R., Molod, A., Takacs, L., ...

- 312 Zhao, B. (2017, June). The Modern-Era retrospective analysis for research and
 313 applications, version 2 (MERRA-2). *J. Clim.*, *30*(Iss 13), 5419–5454.
- 314 Henley, B. J., Gergis, J., Karoly, D. J., Power, S., Kennedy, J., & Folland, C. K.
 315 (2015, December). A tripole index for the interdecadal pacific oscillation.
 316 *Clim. Dyn.*, *45*(11), 3077–3090.
- 317 Hersbach, H., Bell, B., Berrisford, P., Hirahara, S., Horányi, A., Muñoz-Sabater, J.,
 318 ... Thépaut, J. (2020, June). The ERA5 global reanalysis. *Q.J.R. Meteorol.*
 319 *Soc.*, *64*, 29.
- 320 Holloway, C. E., & Neelin, J. D. (2009, June). Moisture vertical structure, column
 321 water vapor, and tropical deep convection. *J. Atmos. Sci.*, *66*(6), 1665–1683.
- 322 Jones, C., & Carvalho, L. M. V. (2006, December). Changes in the activity of the
 323 Madden–Julian oscillation during 1958–2004. *J. Clim.*, *19*(24), 6353–6370.
- 324 Kiladis, G. N., Dias, J., Straub, K. H., Wheeler, M. C., Tulich, S. N., Kikuchi, K.,
 325 ... Ventrice, M. J. (2014). A comparison of OLR and Circulation-Based
 326 indices for tracking the MJO. *Mon. Weather Rev.*, *142*(5), 1697–1715.
- 327 Kiladis, G. N., Straub, K. H., & Haertel, P. T. (2005, August). Zonal and vertical
 328 structure of the Madden–Julian oscillation. *J. Atmos. Sci.*, *62*(8), 2790–2809.
- 329 Knutson, T. R., & Manabe, S. (1995, September). Time-Mean response over the
 330 tropical pacific to increased CO₂ in a coupled Ocean-Atmosphere model. *J.*
 331 *Clim.*, *8*(9), 2181–2199.
- 332 Madden, R. A., & Julian, P. R. (1971, July). Detection of a 40–50 day oscillation in
 333 the zonal wind in the tropical pacific. *J. Atmos. Sci.*, *28*(5), 702–708.
- 334 Madden, R. A., & Julian, P. R. (1972). Description of global-scale circulation cells
 335 in the tropics with a 40–50 day period. *J. Atmos. Sci.*, *29*(6), 1109–1123.
- 336 Maloney, E. D., Adames, Á. F., & Bui, H. X. (2019, January). Madden–Julian oscil-
 337 lation changes under anthropogenic warming. *Nat. Clim. Chang.*, *9*(1), 26–33.
- 338 Maloney, E. D., & Xie, S.-P. (2013, March). Sensitivity of tropical intraseasonal vari-
 339 ability to the pattern of climate warming: MJO ACTIVITY AND CLIMATE
 340 WARMING. *J. Adv. Model. Earth Syst.*, *5*(1), 32–47.
- 341 Mantua, N. J., Hare, S. R., Zhang, Y., Wallace, J. M., & Francis, R. C. (1997,
 342 June). A pacific interdecadal climate oscillation with impacts on salmon pro-
 343 duction*. *Bull. Am. Meteorol. Soc.*, *78*(6), 1069–1080.
- 344 Oliver, E. C. J., & Thompson, K. R. (2012, March). A reconstruction of Madden–
 345 Julian oscillation variability from 1905 to 2008. *J. Clim.*, *25*(6), 1996–2019.
- 346 Sherwood, S. C., & Nishant, N. (2015, May). Atmospheric changes through 2012
 347 as shown by iteratively homogenized radiosonde temperature and wind data
 348 (IUKv2). *Environ. Res. Lett.*, *10*(5), 054007.
- 349 Slingo, J. M., Rowell, D. P., Sperber, K. R., & Nortley, F. (1999). On the pre-
 350 dictability of the interannual behaviour of the Madden-Julian oscillation and
 351 its relationship with el niño. *Quart. J. Roy. Meteor. Soc.*, *125*(554), 583–609.
- 352 Sobel, A. H., & Bretherton, C. S. (2000, December). Modeling tropical precipitation
 353 in a single column. *J. Clim.*, *13*(24), 4378–4392.
- 354 Tao, L., Zhao, J., & Li, T. (2015, November). Trend analysis of tropical intrasea-
 355 sonal oscillations in the summer and winter during 1982–2009: TREND ANAL-
 356 YSIS OF BSISO AND MJO DURING 1982–2009. *Int. J. Climatol.*, *35*(13),
 357 3969–3978.
- 358 Trenberth, K. E., & Stepaniak, D. P. (2001, April). Indices of el niño evolution. *J.*
 359 *Clim.*, *14*(8), 1697–1701.
- 360 Wolding, B. O., & Maloney, E. D. (2015, October). Objective diagnostics and the
 361 Madden–Julian oscillation. part II: Application to moist static energy and
 362 moisture budgets. *J. Clim.*, *28*(19), 7786–7808.
- 363 Wolding, B. O., Maloney, E. D., & Branson, M. (2016, December). Vertically re-
 364 solved weak temperature gradient analysis of the Madden-Julian oscillation in
 365 SP-CESM: WTG ANALYSIS OF THE MJO IN SP-CESM. *J. Adv. Model.*
 366 *Earth Syst.*, *8*(4), 1586–1619.

- 367 Yanai, M., Esbensen, S., & Chu, J.-H. (1973, May). Determination of bulk prop-
368 erties of tropical cloud clusters from Large-Scale heat and moisture budgets. *J.*
369 *Atmos. Sci.*, *30*(4), 611–627.
- 370 Yin, X., Gruber, A., & Arkin, P. (2004, December). Comparison of the GPCP and
371 CMAP merged Gauge–Satellite monthly precipitation products for the period
372 1979–2001. *J. Hydrometeorol.*, *5*(6), 1207–1222.
- 373 Zhang, C. (2013, December). Madden–Julian oscillation: Bridging weather and cli-
374 mate. *Bull. Am. Meteorol. Soc.*, *94*(12), 1849–1870.